Influence of ground motion scaling on floor response spectra

S. P. Challagulla[1,*], B. D. Bhavani[1], A. K. Suluguru[2], Mohammed Jameel[3] and Felipe Vicencio[4]

[1]Department of Civil Engineering, Koneru Lakshmaiah Education Foundation, Vaddeswaram, Guntur District 522 302, India
[2]Department of Civil Engineering, Malla Reddy Engineering College, Maisammaguda 500 100, India
[3]Department of Civil Engineering, College of Engineering, King Khalid University, Asir, Abha, 61421, Saudi Arabia
[4]Facultad de Ingeniería y Tecnología, Universidad San Sebastian, Santiago, Chile

Non-structural components (NSCs) should be analysed properly using the floor response spectra (FRS) method to reduce financial loss due to earthquakes. There are various methods available in the literature to scale recordings. However, there is little or no agreement among researchers regarding the correctness of these methods in the analysis of NSCs. Therefore, the present study examines the influence of different amplitude scaling techniques (geometric mean and Sa(T_1)) and spectral matching procedures on the seismic demands of NSCs. The spectral matching method shows the lowest ground motion parameter dispersion. The results reveal that the Sa(T_1) scaling method produces lower floor responses. The spectral matching method shows smaller dispersion in the spectral ordinates and median response quantities. The amplification factors estimated in this study were compared to those from the existing code formulations. Based on the findings of this study, the spectral matching approach in the time domain may be utilized to better estimate seismic demands on NSCs.

Keywords: Amplitude scaling, dispersion, floor amplification, non-structural components, spectral matching.

NON-STRUCTURAL components (NSCs) are associated with the building structure but do not resist loads[1]. Damage to NSCs may cause greater direct and indirect economic loss than structural members[2]. Compared to structural elements, the seismic design of NSCs is not well-documented. The current standards and guidelines are based on empirical methodology[3]. Therefore, NSCs must be designed to withstand earthquakes. For this, the floor acceleration spectra at the point where the NSC is mounted to the primary structure should be determined.

The floor response spectra (FRS) approach is a decoupled analysis method[4]. FRS can be generated using time-history analysis[5]. The main structure is dynamically analysed first, and then the acceleration response history of NSC is fed to a secondary structure to generate FRS. A set of ground motions (amplitude-scaled) with their average response spectrum in accordance with the target spectrum can be used. An alternative method involves modifying the shape of the response spectrum to match the spectrum of a target site via wavelet addition in the time domain. Some studies found that amplitude-scaled ground motion scale factors can contribute to a biased assessment of mean structural responses[6], whereas others found the reverse trend. The present study aims to generate the FRS for different amplitude-scaling and spectral-matching methods. The NSCs considered in this study are acceleration-sensitive. They are mounted on the floors, ceilings or walls of the building structure and are therefore susceptible to enhanced seismic ground vibrations generated by the filtering action of the building structure. The floor amplification factors are crucial in determining the seismic demands on NSCs and are evaluated under different scaled ground motions.

Modelling of a building

A four-storey reinforced concrete building was considered for this study (Figure 1). The building has a 3D special moment-resisting bare frame. The structure is assumed to be located in the highest seismic zone (Zone V, according to IS 1893-2016). All floors have a constant bay width of 4 m and a storey height of 3 m. Grades of concrete and steel are M 30 and HYSD 415. Floor finishes and live load were set at 1.5 and 3 kN/m^2 respectively, according to relevant Indian standards.

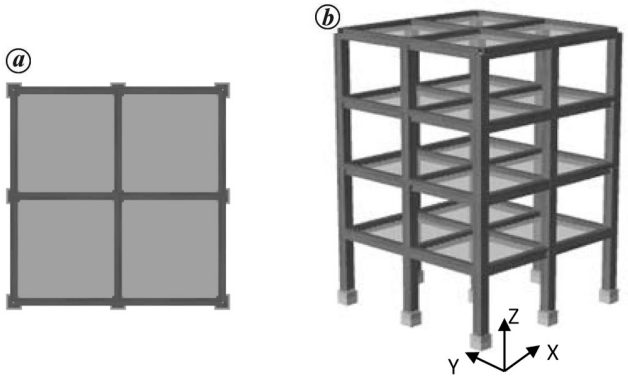

Figure 1. Building model considered: (***a***) typical building plan and (***b***) 3D model.

*For correspondence. (e-mail: chsuryaprakash@kluniversity.in)

The beam size (300 mm × 450 mm) and column size (450 mm × 450 mm) were kept uniform throughout the building. The RCC slab was 150 mm thick. The building model was developed using the software SeismoStruct[7]. The compression behaviour of confined concrete was according to the model developed by Mander *et al.*[8]. The tension behaviour of steel reinforcement was accounted for using Menegotto–Pinto steel model[9].

A Rayleigh damping model of 5% (associated with the first two modes in the X direction) was defined to model the damping effects as shown in eq. (1).

$$C = \alpha_{\mathrm{m}} M + \alpha_k K, \tag{1}$$

where the proportionality constants α_{m} and α_k are the mass and stiffness proportionality damping with units second^{-1} and second respectively, and M, K and C, are the mass, stiffness, and damping matrices respectively. α_{m} and α_k can be calculated using eqs (2) and (3).

$$\alpha_{\mathrm{m}} = 4\pi \frac{\xi_1 T_1 - \xi_2 T_2}{T_1^2 - T_2^2}, \tag{2}$$

$$\alpha_k = \frac{T_1 T_2}{\pi} \frac{\xi_2 T_1 - \xi_1 T_2}{T_1^2 - T_2^2}, \tag{3}$$

where T_1, T_2 are the vibration periods and ξ_1, ξ_2 are the damping ratios of the building structure associated with modes 1 and 2 respectively. Table 1 shows the dynamic characteristics of the considered building model. The vibration period of the NSC is represented as T_s. The ground motions are used to conduct the primary structural dynamic analysis. Then, the absolute acceleration response of the structure at a given floor level is fed into a single-degree-of-freedom (SDOF) system to construct the FRS.

Selection of ground motion

Twenty horizontal unscaled real ground motions were considered from the Pacific Earthquake Engineering Research Centre (PEER) NGA-West2 Database (Table 2). In this study, the vertical component of the ground motions has been neglected. According to the National Earthquake Hazard Reduction Program (NEHRP) site classification system, excitations are chosen based on shear wave velocity (V_{S30}) to represent hard soil. The effect of a strong pulse caused by forward directivity is beyond the scope of this study. The response spectrum consistent with hard soil and zone V, according to IS 1893: 2016, was considered the target spectrum. Figure 2 shows the Fourier amplitude spectra (acceleration) of the ground motions. From the figure, it can be observed that all the excitations show significant wide-range frequency content. Two ground motions, viz. Parkfield and Northern Claif-07 show a peak frequency of approximately 2.4 Hz, which is in the vicinity of the fundamental frequency of the building (2.49 Hz).

Table 1. Time period (modal) and modal mass participation ratio of the building

Mode	Period of vibration (sec)	Modal mass participation ratio (%)
1	0.401	80.5
2	0.127	10.5
3	0.071	1.50

Ground motion scaling techniques

Method 1: Geometric-mean or MSE scaling

The mean square error (MSE) measures the difference between the spectral acceleration of a recording and the target spectrum. It was computed using eq. (4) below according to PEER documentation.

$$\mathrm{MSE} = \frac{\sum_i w(T_i)\{\ln[\mathrm{Sa}_{\mathrm{target}}(T_i)] - \ln[f * \mathrm{Sa}_{\mathrm{response}}(T_i)]\}^2}{\sum_i w(T_i)}, \tag{4}$$

where $w(T_i)$ is the weight function used to assign various weights to distinct periods of interest, $\mathrm{Sa}_{\mathrm{target}}(T_i)$ is the spectral acceleration of a target response spectrum at time period T_i, $\mathrm{Sa}_{\mathrm{response}}(T_i)$ is the spectral acceleration of the record response spectra, and f is a scale factor assigned to the complete response spectrum of the recording. Table 3 shows the scale factors and associated MSE values of the ground motions. Figure 3 *a* shows the response spectra of the scaled ground motions.

Method 2: Sa(T_1) scaling

In the initial mode period of a structure, amplitude scaling of the recordings to a defined spectral acceleration is used. The unscaled records were adjusted to match the target spectral acceleration. Figure 3 *b* depicts the adjusted time histories. Table 3 shows the scale factors of the ground motions. The spectral acceleration dispersion was relatively significant in the mid- and short-period regions (Figure 3 *b*).

Method 3: Spectral matching in the time domain

The spectral matching method in the time domain involves adding and subtracting basic wavelets from the original ground motion signal. The mean spectral ordinates for methods 1 and 2 were not in good agreement with those from the target spectrum in the range between 0.1 and 0.4 sec, and also in the mid-period range (Figure 3 *a* and *b*). The

Table 2. Details of unscaled real ground motions

Earthquake	Year	Station	M_w	R_{rup} (km)	V_{s30} (m/s)
Kern County	1952	Santa Barbara Courthouse	7.36	82.19	514.99
Kern County	1952	Taft Lincoln School	7.36	38.89	385.43
Parkfield	1966	Temblor pre-1969	6.19	15.96	527.92
Lytle Creek	1970	Wrightwood – 6074 Park Dr	5.33	12.14	486
San Fernando	1971	Castaic – Old Ridge Route	6.61	22.63	450.28
San Fernando	1971	Lake Hughes #1	6.61	27.4	425.34
San Fernando	1971	Lake Hughes #12	6.61	19.3	602.1
San Fernando	1971	Palmdale Fire Station	6.61	28.99	452.86
San Fernando	1971	Pasadena – CIT Athenaeum	6.61	25.47	415.13
San Fernando	1971	Santa Felita Dam (Outlet)	6.61	24.87	389
Northern Calif-07	1975	Petrolia_General Store	5.2	34.67	368.72
Friuli_Italy-01	1976	Tolmezzo	6.5	15.82	505.23
Friuli_Italy-02	1976	Forgaria Cornino	5.91	14.75	412.37
Santa Barbara	1978	Santa Barbara Courthouse	5.92	12.16	514.99
Tabas_Iran	1978	Dayhook	7.35	13.94	471.53
Coyote Lake	1979	Coyote Lake Dam	5.74	6.13	561.43
Coyote Lake	1979	Gilroy Array #6	5.74	3.11	663.31
Norcia_Italy	1979	Cascia	5.9	4.64	585.04
Imperial Valley-06	1979	Cerro Prieto	6.53	15.19	471.53
Livermore-01	1980	Del Valle Dam (Toe)	5.8	24.95	403.37

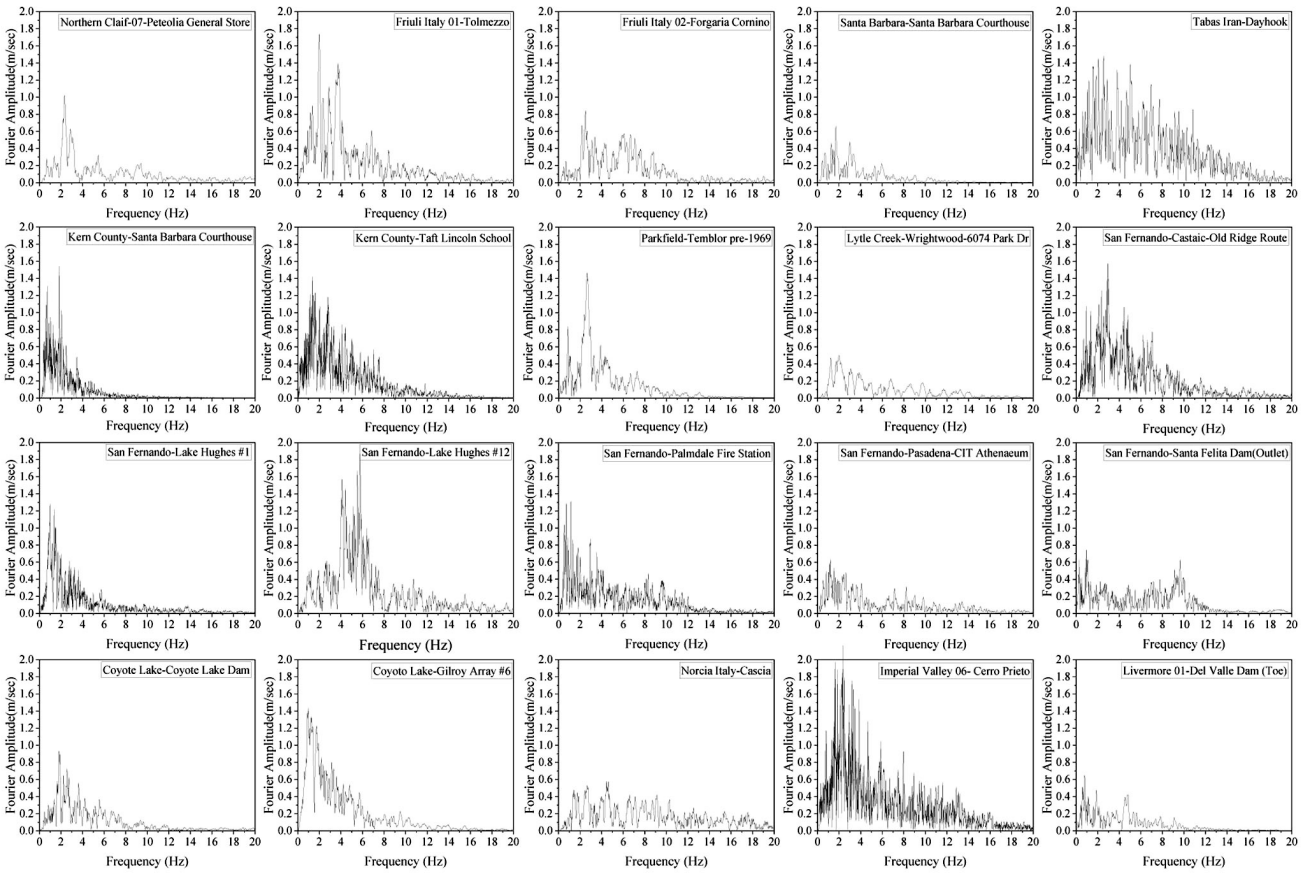

Figure 2. Fourier amplitude spectra of ground motions.

spectrally matched ground motions were generated using the program SeismoMatch[10]. From Figure 3 *c*, it can be observed that the mean and target spectra show good agreement for the whole period.

Unscaled and scaled ground motion parameters

Prior to assessing the structural system, potential damage indicators were used to evaluate the scaled ground motions.

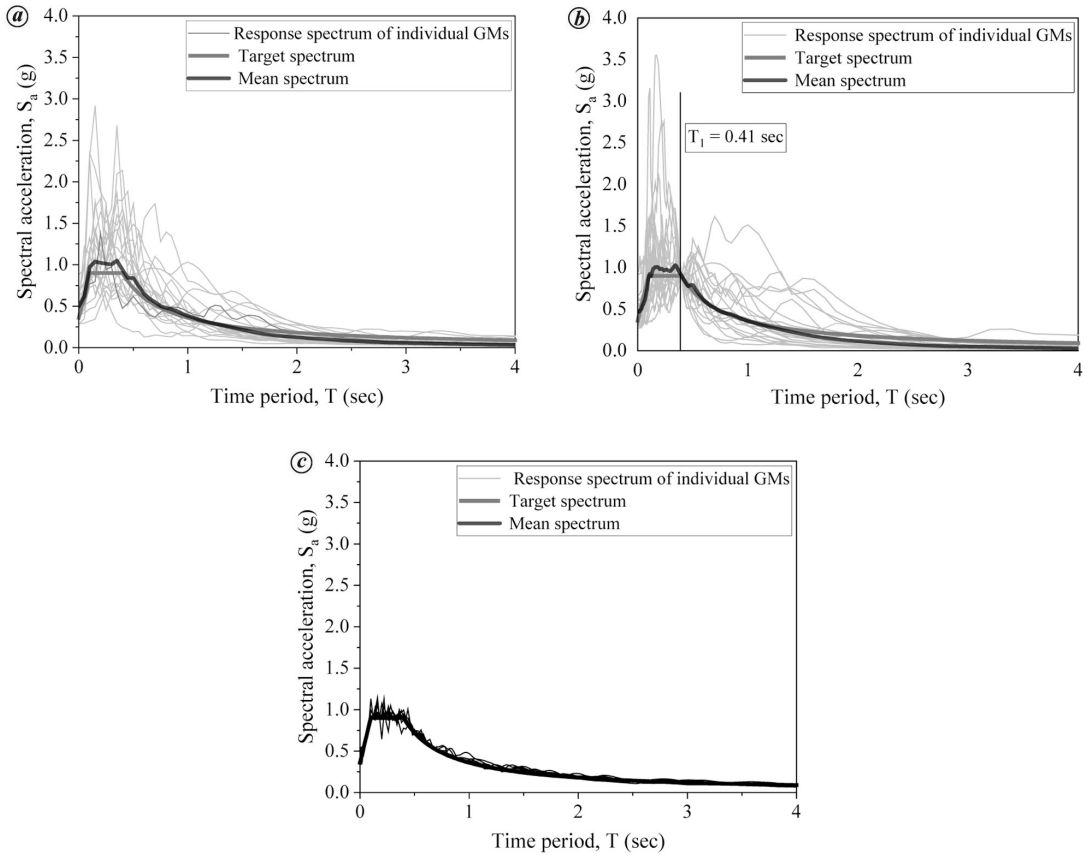

Figure 3. Response spectra of scaled ground motions: (***a***) MSE, (***b***) Sa(T_1) and (***c***) spectral matching.

Table 3. Scale factors of ground motion for MSE and Sa(T_1) scaling methods

Earthquake	MSE	Sa(T_1)
Kern County	3.230	3.557
Kern County	2.124	2.423
Parkfield	1.954	0.827
Lytle Creek	4.301	3.224
San Fernando	2.043	1.723
San Fernando	2.695	3.975
San Fernando	2.557	2.430
San Fernando	2.476	4.028
San Fernando	3.669	4.218
San Fernando	3.191	4.272
Northern Calif-07	3.538	1.801
Friuli_Italy-01	1.515	1.227
Friuli_Italy-02	3.373	1.822
Santa Barbara	4.475	6.132
Tabas_Iran	1.270	1.451
Coyote Lake	3.572	2.214
Coyote Lake	1.158	1.280
Norcia_Italy	4.435	2.523
Imperial Valley-06	1.996	1.611
Livermore-01	3.690	7.044

These indicators depict several time-related characteristics. The indicators used were as follows:

- Peak ground acceleration (PGA).
- Root mean square of acceleration (RMSA):

$$\text{RMSA} = \sqrt{\frac{1}{t_\text{d}} \int_0^{t_\text{d}} [a(t)]^2 \, \text{d}t}, \tag{5}$$

where $a(t)$ is the acceleration at time t and t_d is the total duration of ground motion.

- Arias intensity (AI):

$$\text{AI} = \frac{\pi}{2g} \int_0^{t_\text{d}} a^2(t) \text{d}t, \tag{6}$$

where g is the acceleration due to gravity.

- Cumulative absolute velocity (CAV):

$$\text{CAV} = \int_0^{t_\text{d}} | a(t) | \, \text{d}t. \tag{7}$$

The GMPs (RMSA, AI and CAV), as defined in eqs (5)–(7), were determined for all the unscaled (original) and scaled ground motions. Figure 4 shows their mean and standard deviations.

The following observations can be made from Figure 4: (i) Even though spectrum-matched time histories match the

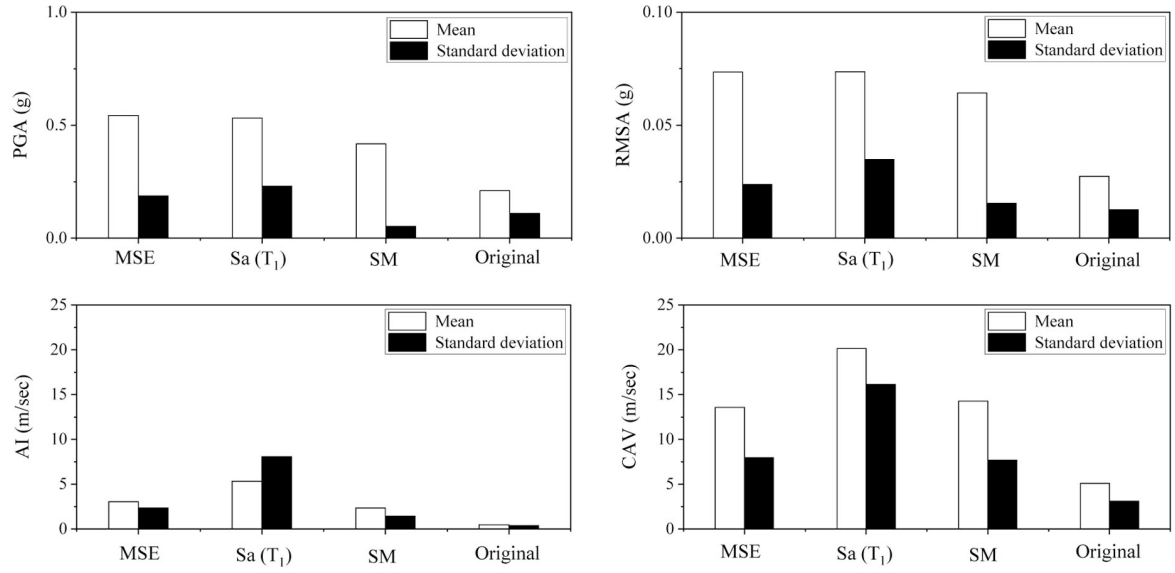

Figure 4. Comparison of mean of various ground motion parameters.

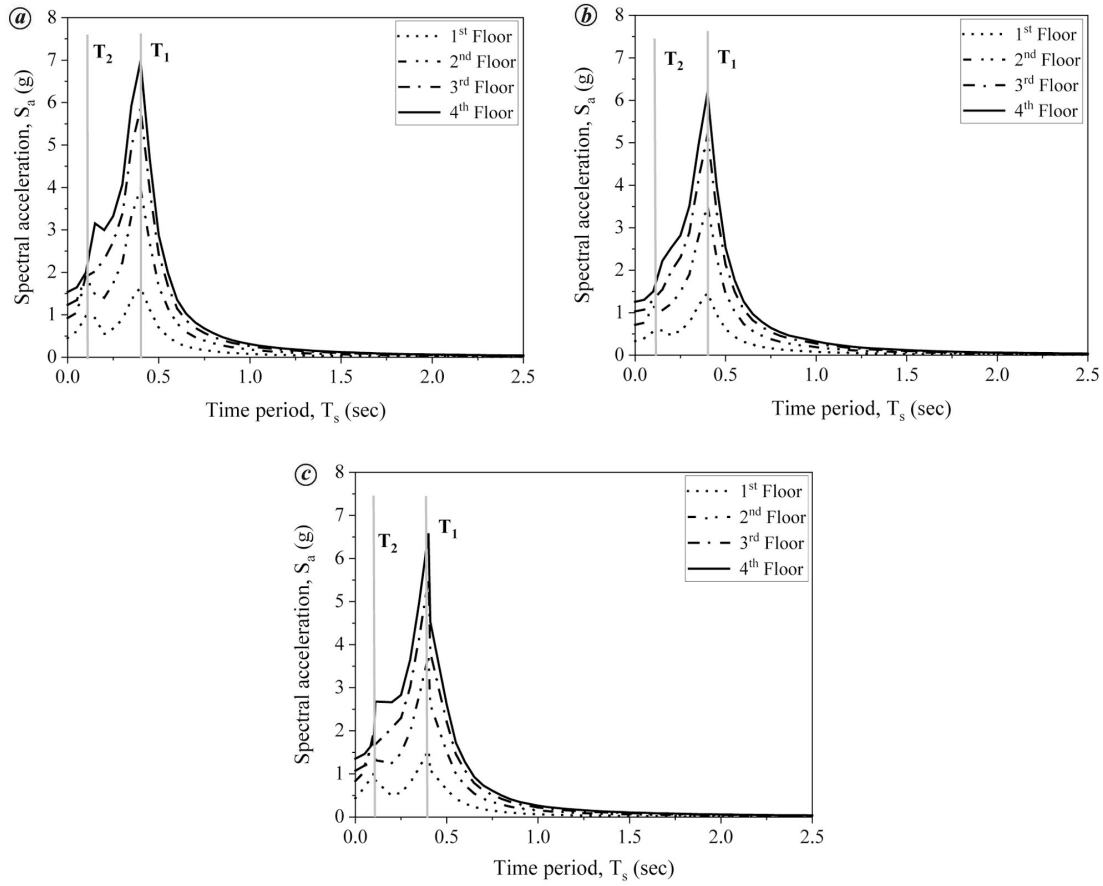

Figure 5. Mean floor response spectra: (***a***) method 1, (***b***) method 2 and (***c***) method 3.

desired response spectrum, mean GMPs are different. (For example, mean PGA is two times greater than PGA measured by unscaled ground motions.) (ii) Scaling and spectral matching yield substantial ground motions for all GMPs. (iii) Spectral matching reduces AI, PGA and RMSA. (iv) Method 3 has the lowest damage indication standard deviation.

According to these findings, spectral matching using the time domain approach is the most reliable method since it

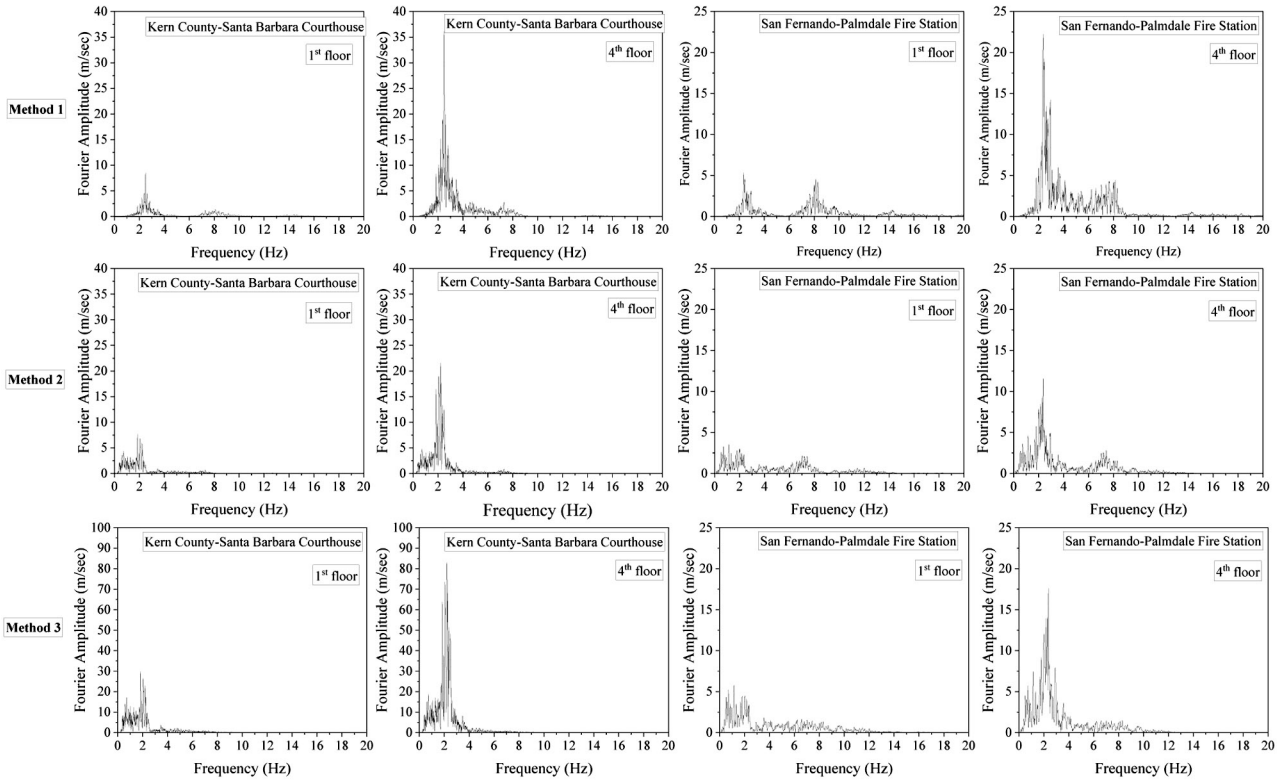

Figure 6. Fourier amplitude spectra of floor accelerations.

yields satisfactory results for PGA, RMSA, AI and CAV while preserving a small dispersion. Similar findings can be found in the literature[11].

Results of analysis

Floor response spectrum

Here we present analysis results in the form of FRS. Linear time-history analysis (LTHA) was performed in this study since it is commonly used to evaluate the dynamic behaviour of structures and their components. LTHA was conducted on the structure when subjected to different scaled ground motions in the *X*-direction. Elastic FRS for each scaled ground motion at different floor levels were obtained. Figure 5 shows the mean FRS.

From Figure 5, it can be observed that various peaks in the FRS correspond to different fundamental modes of the building. The two peaks observed in the FRS were recorded close to the elastic modal periods of the structure (Table 1). This finding is consistent with the outcomes of a previous study[12]. The peaks in the FRS were due to the resonance effect and can be seen from the Fourier amplitude spectra of floor accelerations (Figure 6) (first and fourth floors). In Figure 6, a sharp peak (2.42 Hz) can be observed on the top floor, which coincides with the fundamental frequency of the building (2.49 Hz). From the lowest to the highest floors, the FRS evaluations for different scaling methods revealed a gradual increase in response[13]. Table 4 presents the median of peak floor acceleration (PFA), spectral acceleration (Sa), and dispersion (standard deviation) in the response of the building at the first and fourth-floor levels. The seismic demands on secondary systems are represented by floor spectral acceleration.

From Table 4, it can be observed that method 2 yields the lowest estimate of median floor acceleration. This is because the recordings are only adjusted to the spectrum (target) at the first period of the structure. As a result, the spectral acceleration dispersion at higher frequencies is fairly significant (Figure 3 *b*). The standard deviation in spectral ordinates for method 1 is greater than that for method 3 at high frequencies (Figure 3 *a* and *c*). As a result, method 1 has a wider dispersion in peak floor acceleration than method 3. Table 4 shows that the Sa(T_1) technique yields a lower peak floor acceleration than the MSE method. From Figure 3 *c* and Table 4, it can be observed that the spectral matching method shows smaller dispersion in the spectral ordinates and peak floor acceleration. The floor spectral acceleration is often similar to the peak floor acceleration described above (Table 4). As a result, ground motion modification using the spectrum matching approach allows for a more precise calculation of peak and spectral accelerations on the floor. Method 2 may be avoided for estimating the response of NSCs, which might result in a lower estimate.

Table 4. Median response and their dispersion of a building model

Parameter	Floor level	Median response			Dispersion		
		Method 1	Method 2	Method 3	Method 1	Method 2	Method 3
PFA (g)	1	0.463	0.321	0.440	0.256	0.124	0.062
	4	1.632	1.225	1.350	0.627	0.521	0.130
Sa@ T_1 (g)	1	1.592	1.568	1.618	0.938	0.694	0.303
	4	6.752	6.553	6.651	3.997	2.905	1.271
Sa@ T_2 (g)	1	1.030	0.554	0.839	0.464	0.360	0.133
	4	3.439	1.973	2.575	1.821	1.432	0.367

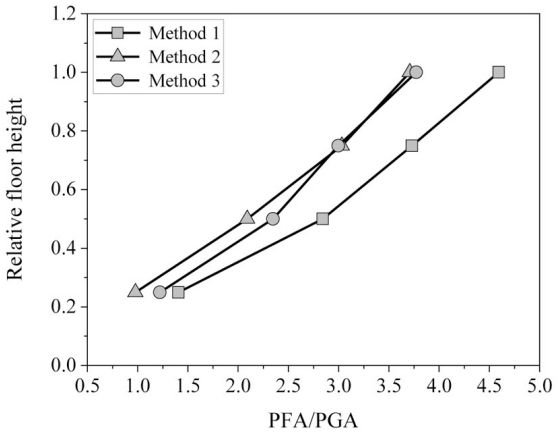

Figure 7. Normalized floor amplification factors of a building structure.

Floor amplification factor

The normalized floor amplification factor was evaluated to study the effect of different scaling techniques on the peak floor response throughout the height of the building. It is the ratio between the absolute maximum/PFA and PGA. Several codes exist to assess the variation of PFA along with the height of the structure. The definition of floor amplification factor in different seismic codes like ASCE 7-16 (ref. 14), Eurocode 8 (ref. 15), and GB 50011-2010 (ref. 16) is given by eq. (8), (9) and (10) respectively. PFA varies linearly along with the height of a building (Figure 7). Floor amplification factors were estimated to be larger for method 1 than for the other methods.

$$\text{PFA/PGA} = 1 + 2\frac{z}{h}, \tag{8}$$

$$\text{PFA/PGA} = 1 + 1.5\frac{z}{h}, \tag{9}$$

$$\text{PFA/PGA} = 1 + \frac{z}{h}. \tag{10}$$

Figure 8 compares current floor amplification factors with those obtained from the existing codes. Except at the first-floor level, method 1 overestimates PFA demands compared to those computed from the codes (Figure 8 *a*). Method 2 underestimates PFA demand on the first floor and overestimates it on the subsequent floors (Figure 8 *b*). Method 3 underestimates peak floor demands compared to ASCE 7-16 and Eurocode 8 (Figure 8 *c*). The peak floor response for the remaining floor levels is overestimated. It can be inferred from Figure 8 that PFA demands computed from ASCE 7-16 are comparatively close to those determined by different scaling techniques. From eqs (8)–(10), it can be concluded that the peak floor demands are independent of the vibration period of the building. In general, the PFA response depends on various dynamic characteristics of a building[4,5]. Hence, in this study, we have compared the floor amplification factors obtained for different scaling techniques with those obtained from the period-dependent codes.

Figure 9 compares the floor amplification factors obtained in the present study with those obtained from the formulation proposed by the Applied Technology Council (ATC), USA. Such a formulation can be seen in eqs (11)–(14).

$$\text{PFA/PGA} = 1 + a_1\left[\frac{z}{h}\right] + a_2\left[\frac{z}{h}\right]^{10}, \tag{11}$$

$$a_1 = \frac{1}{T_{\text{abldg}}} \le 2.5, \tag{12}$$

$$a_2 = \left[1 - \left(\frac{0.4}{T_{\text{abldg}}}\right)^2\right] > 0, \tag{13}$$

where T_{abldg} is the fundamental period according to ASCE/SEI 7-16 and is calculated as follows:

$$T_{\text{abldg}} = C_t h_n^x, \tag{14}$$

where h_n is the height of the building (m) and the coefficients C_t and x are determined from table 12.8-2 of ASCE/SEI 7-16.

The approximate building period considered in this study was calculated using eq. (14) was found to be 0.431 sec, nearly equal to the actual period of the building (T_1) with a

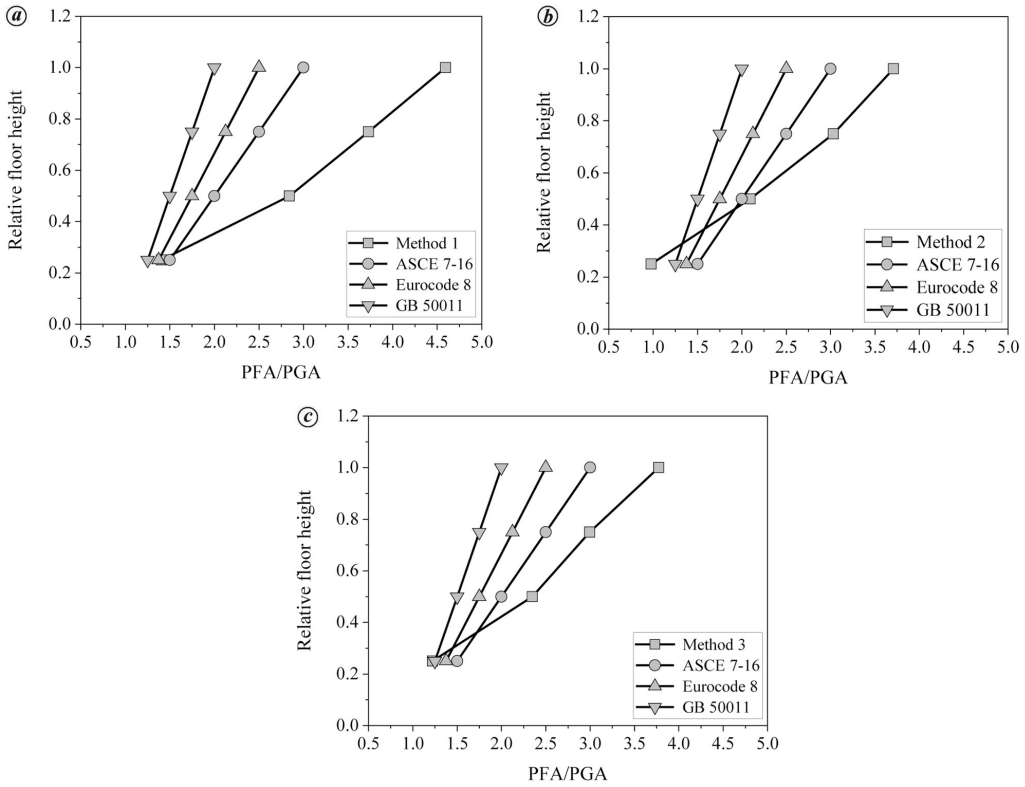

Figure 8. Comparison of floor amplification factors: (***a***) method 1, (***b***) method 2 and (***c***) method 3.

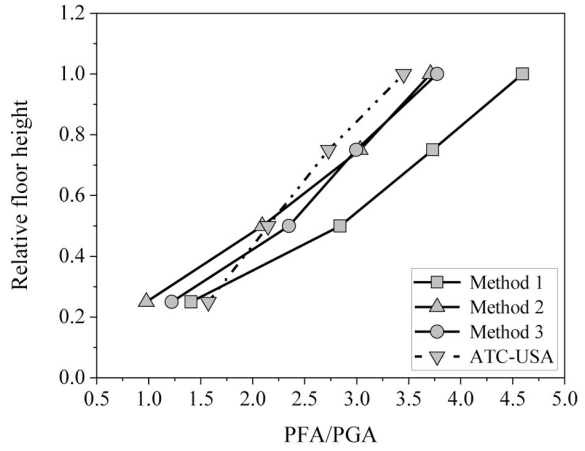

Figure 9. Comparison of floor amplification factors between the building and ATC, USA.

7.48% difference. Compared to the ATC formulation, method 1 overestimates the PFA/PGA values (Figure 9). Compared to method 2, method 3 provides results closer to the ATC formulation at all floor levels.

Component amplification factor

To study the component acceleration amplification of the floor acceleration, a parameter known as the component amplification factor is defined in this study. It measures the ratio between the maximum floor spectral acceleration (FSA_{max}) and PFA. Figure 10 shows the trend in the component acceleration amplification with respect to floor height.

From Figure 10, it can be observed that the component amplification factors vary from 3.24 to 4.39 in method 1, 4.12 to 4.76 in method 2 and 3.52 to 5.13 in method 3. The trends are comparable to the regulations in ASCE7 and EC8, which specify a trend that ranges from 2.5 at the base of the structure to 2.5 and 2.2 at the top for ASCE 7-16 and Eurocode 8 respectively. Therefore, as demonstrated by Medina *et al.*[17], a notable underestimation of the component amplification factors in the current building codes is well established. The maximum value of the component amplification factor for a four-storey building model observed in this study of Shang *et al.*[18] and the present study is 5.72 and 5.13 (from method 3) respectively. The observed difference between the values is due to the different building dynamic characteristics and ground motions. The component amplification factors varied from 3.0 to 5.2 for the elastic building models[19]. A similar range was obtained in the present study utilizing the ground motions obtained in method 3.

Summary and conclusion

The present study evaluated different scaling techniques of ground motions on seismic demands of NSCs. The building

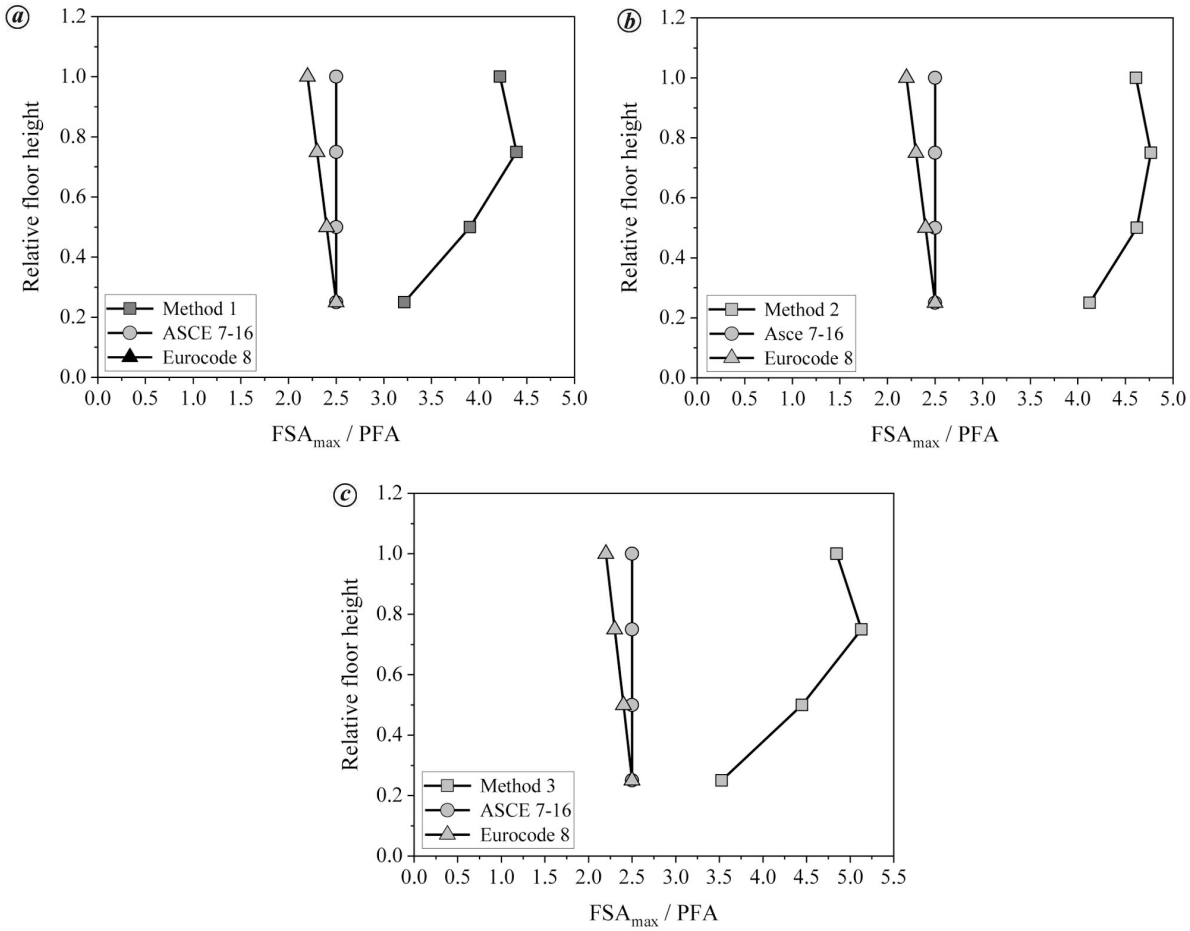

Figure 10. Comparison of component amplification factors: (***a***) method 1, (***b***) method 2 and (***c***) method 3.

model considered was a four-storey regular reinforced concrete framed structure. The following specific conclusions can be drawn from this study.

- The lowest standard deviation (dispersion) of the damage indicators among the three approaches can be observed in method 3.
- Compared to the other methods, method 2 provides the lowest estimation of median response.
- The spectral matching method (method 3) shows smaller dispersion in the spectral ordinates and median response than the amplitude scaling methods.
- The code-based floor amplification formulations may lead to overestimation (first floors) and underestimation (second to fourth floors) of peak floor response.
- The floor amplification factors depend on the vibration period of the building model. Method 3 shows good agreement with the ATC-USA formulation.
- Method 3 accurately evaluates the component acceleration amplification throughout the building height.

Conflict of interest: The authors declare that there is no conflict of interest.

1. Filiatrault, A. and Sullivan, T., Performance-based seismic design of nonstructural building components: the next frontier of earthquake engineering. *Earthq. Eng. Eng. Vib.*, 2014, **13**, 17–46.
2. Di Sarno, L., Magliulo, G., D'Angela, D. and Cosenza, E., Experimental assessment of the seismic performance of hospital cabinets using shake table testing. *Earthq. Eng. Struct. Dyn.*, 2019, **48**, 103–123.
3. Anajafi, H. and Medina, R. A., Evaluation of ASCE 7 equations for designing acceleration-sensitive nonstructural components using data from instrumented buildings. *Earthq. Eng. Struct. Dyn.*, 2018, **47**, 1075–1094.
4. Challagulla, S. P., Bhargav, N. C. and Parimi, C., Evaluation of damping modification factors for floor response spectra via machine learning model. *Structures*, 2022, **39**, 679–690.
5. Surana, M., Singh, Y. and Lang, D. H., Effect of irregular structural configuration on floor acceleration demand in hill-side buildings. *Earthq. Eng. Struct. Dyn.*, 2018, **47**, 2032–2054.
6. Du, W., Ning, C. L. and Wang, G., The effect of amplitude scaling limits on conditional spectrum-based ground motion selection. *Earthq. Eng. Struct. Dyn.*, 2019, **48**, 1030–1044.
7. SeismoStruct – A computer software program for static and dynamic nonlinear analysis of framed structures, 2020.
8. Mander, J. B., Priestley, M. J. N. and Park, R., Theoretical stress–strain model for confined concrete. *J. Struct. Eng.*, 1988, **114**, 1804–1826.
9. Menegotto, M., Method of analysis for cyclically loaded RC plane frames including changes in geometry and non-elastic behavior of elements under combined normal force and bending. In Proceedings of

the IABSE Symposium on Resistance and Ultimate Deformability of Structures Acted on by Well Defined Repeated Loads, 1973, pp. 15–22.
10. SeismoMatch – A computer program for spectrum matching of earthquake records, 2020.
11. Li, B. and Zhou, Y., Assessment of spectrum-matched time histories for floor response spectra generation. *Structures*, 2022, **38**, 123–138.
12. Landge, M. V. and Ingle, R. K., Comparative study of floor response spectra for regular and irregular buildings subjected to earthquake. *Asian J. Civ. Eng.*, 2021, **22**, 49–58.
13. Uma, S. R., Zhao, J. X. and King, A. B., Seismic actions on acceleration sensitive non-structural components in ductile frames. *Bull. N.Z. Soc. Earthq. Eng.*, 2010, **43**, 110–125.
14. ASCE/SEI 7-16, Minimum design loads for buildings and other structures. American Society of Civil Engineers, Virginia, USA, 2017.
15. CEN. Eurocode 8. Design of structures for earthquake resistance. Part 1: General rules, seismic actions and rules for buildings, CEN, Brussels, Belgium, 2004.
16. GB 50011-2010. Code for seismic design of buildings. Ministry of Housing and Urban–Rural Construction of the People's Republic of China, 2010.
17. Medina, R. A., Sankaranarayanan, R. and Kingston, K. M., Floor response spectra for light components mounted on regular moment-resisting frame structures. *Eng. Struct.*, 2006, **28**, 1927–1940.
18. Shang, Q., Li, J. and Wang, T., Floor acceleration response spectra of elastic reinforced concrete frames. *J. Build. Eng.*, 2022, **45**, 103558.
19. Petrone, C., Magliulo, G. and Manfredi, G., Seismic demand on light acceleration-sensitive nonstructural components in European reinforced concrete buildings. *Earthq. Eng. Struct. Dyn.*, 2015, **44**, 1203–1217.

ACKNOWLEDGEMENT. We thank the Deanship of Scientific Research at King Khalid University, Saudi Arabia for providing funds to carry out this study through large group project under grant number RGP.2/93/43.

Received 30 June 2022; revised accepted 17 January 2023

doi: 10.18520/cs/v124/i8/928-937